Available online at www.sciencedirect.com
ScienceDirect
Journal of Power Sources 162 (2006) 1351–1356
JOURNAL OF POWER SOURCES
www.elsevier.com/locate/jpowsour

Short communication

Influence of the microstructure on the electrochemical performance of thin film WO_3 cathode

R. Figueroa [a], M. Kleinke [a], Tersio G.S. Cruz [b], A. Gorenstein [a,*]

[a] *Applied Physics Department, Physics Institute, UNICAMP, CP 6165, CEP 13083-970 Campinas, SP, Brazil*
[b] *Telecommunication Technological Division, CESET/UNICAMP, CEP 13484-370 São Paulo, SP, Brazil*

Received 13 July 2006; received in revised form 31 July 2006; accepted 1 August 2006
Available online 12 September 2006

Abstract

In this work, WO_3 thin films deposited at different powers and geometries have been evaluated for use as electrodes in thin film batteries. The potential profiles and cycling capacity in lithium electrolyte were investigated. The discharge capacity for samples strongly depends on the deposition conditions, and there is a clear correlation between microstructure and electrochemical performance.
© 2006 Elsevier B.V. All rights reserved.

Keywords: Tungsten oxide; Reactive sputtering; Thin films; Microbatteries

1. Introduction

In electrochemical devices such as lithium-ion microbatteries [1–5] and electrochromic devices [6,7] the cathode is present in thin film form. Most of the scientific and technological investigations are directed to the development of new cathode compounds [2,8–12] with optimized performance. Transition metal oxide thin films are among the most studied materials, and the deposition technique and deposition parameters are determinant in the performance of the device. In contrast, the present work is centered in exploring new film architectures, as a conceptual method for fabricating the optimized cathodes.

Physical vapor deposition (PVD) techniques as thermal evaporation or sputtering, with the substrate inclined with respect to the vapor source (oblique angle deposition) can produce very interesting structures [13]. On the other hand, other deposition parameters, as the applied power during deposition, can alter the film microstructure. In this paper, we report on the intercalation properties of WO_3 thin films obtained by rf sputtering at different powers, either with the substrate at normal incidence or inclined with respect to the incoming flow. The aim of the work is to investigate the dependence of the charge capacity on these parameters, since this could be a very simple method to optimize the behavior of thin film electrodes.

2. Experimental

The thin films have been prepared by reactive rf magnetron sputtering using a BAE 250 equipment. The WO_3 thin films were deposited using a tungsten target (50 mm diameter) in an Ar/O_2 reactive atmosphere. The Ar/O_2 flow ratio was adjusted in order to obtain the desired film composition (WO_3). The total pressure during deposition was 4.5×10^{-3} mbar and the target-substrate distance (center to center) was 120 mm. A scheme of the geometry is shown in Fig. 1. Substrates were glass covered with indium-tin oxide (ITO) or Si, positioned at angles $\alpha = 0^\circ$ (substrate normal to the sputtered incident flow) or $\alpha = 70^\circ$ (oblique incidence). rf power was varied between 60 and 200 W. Table 1 presents the main deposition conditions.

In order to determine the film deposition rate and provide electrical contacts for electrochemical measurements, a thin, vacuum-friendly, polymeric adhesive tape was used to shield part of the substrate surface during deposition. Thickness was measured using an Alpha-Step 200 profilometer.

W and O contents were obtained by Rutherford scattering spectroscopy (RBS) using a 2.2 MeV He^+ beam. The presence of crystalline phases was investigated by X-ray diffraction (XRD)

* Corresponding author. Tel.: +55 19 37885411; fax: +55 19 37885376.
E-mail address: annette@ifi.unicamp.br (A. Gorenstein).

0378-7753/$ – see front matter © 2006 Elsevier B.V. All rights reserved.
doi:10.1016/j.jpowsour.2006.08.002

Table 1
Deposition conditions

Deposition angle (°)	rf power (W)	Oxygen flow (sccm)	Argon flow (sccm)	Thickness (nm)
0	60	3.9	28.2	249
0	100	5.5	27.2	243
0	150	7.5	23.3	236
0	200	10.0	21.6	240
70	60	2.5	30.8	258
70	100	4.0	35.8	334
70	150	6.0	26.7	335
70	200	8.0	25.2	236

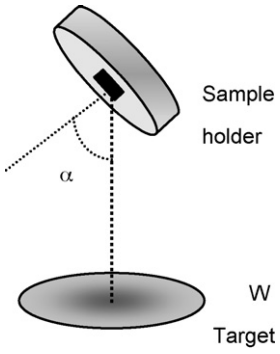

Fig. 1. Scheme of the sputtering geometry.

using a θ–θ RINT 2100/ULTIMA diffractometer, and a 3 kW Rigaku generator, with Cu Kα radiation.

The surface morphology was studied by atomic force microscopy (AFM). The images were obtained with an Auto-Probe CP of ThermoMicroscope, operating in contact mode. Morphologies of surface and cross-sections of the films were observed using a scanning electron microscope (SEM) FEG JSM 6330F.

The electrochemical properties (mainly charge capacity) were investigated using chronopotentiometry with potential limitation. The thin films were tested in about 50 charge/discharge cycles, using propylene carbonate with 1 M lithium perchlorate (PC/$LiClO_4$) as electrolyte. Two lithium foils were used as counter and reference electrodes. The experiment was performed within the potential limits 4.0 to −2.0 V versus Li, under a current density of 5 μA cm^{-2}. The equipment was a multipotentiostat VMP (Biologics). All measurements were performed maintaining the electrochemical cell inside an Ar-filled dry box.

3. Results and discussion

Fig. 2 presents the deposition rate as a function of power, for the two geometries. As expected, the deposition rate increases with the increase of power. As a consequence, the oxygen flow during deposition has to increase (Fig. 3), in order to attain the desired sample composition. Fig. 4 presents the O/W ratio, for samples deposited at different rf power ($\alpha = 0^\circ$, normal deposition). The data was obtained by simulating the RBS profile using the software RUMP [14]. A slight decrease of the ideal composition ([O/W]=3) is observed with the increase of the power. Also,

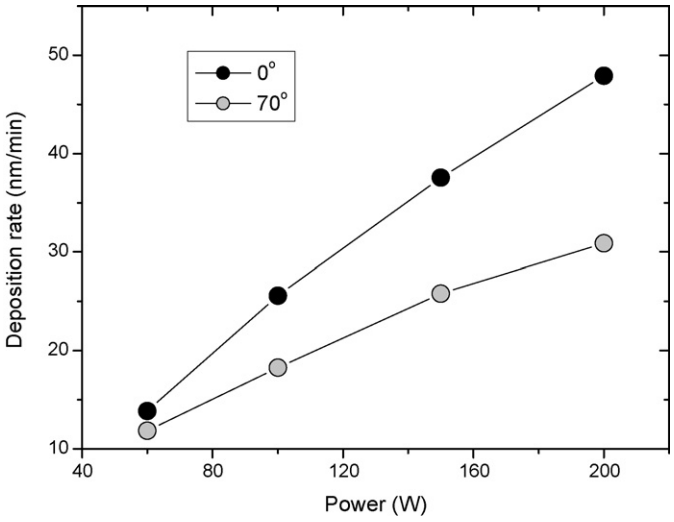

Fig. 2. Deposition rate as a function of power.

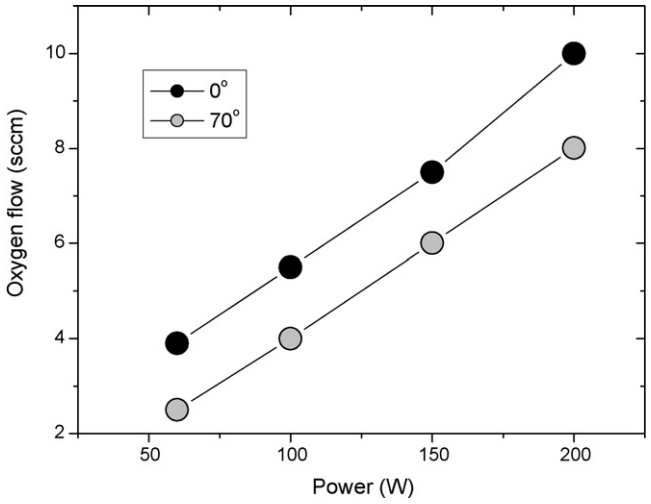

Fig. 3. Oxygen flow during deposition vs. power.

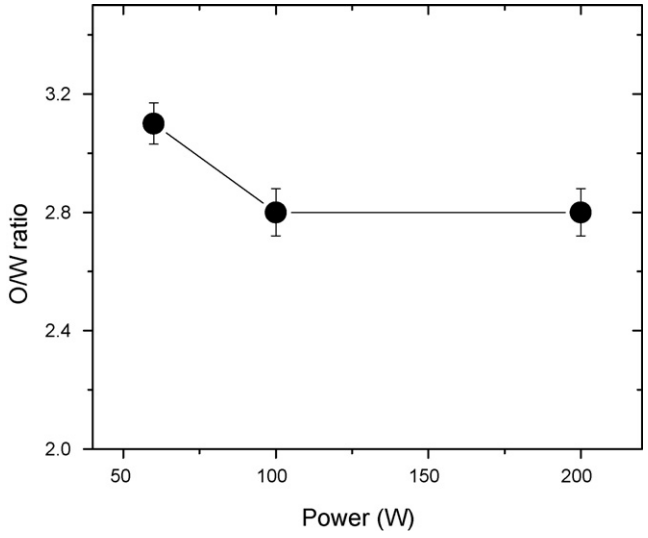

Fig. 4. O/W ratio vs. power.

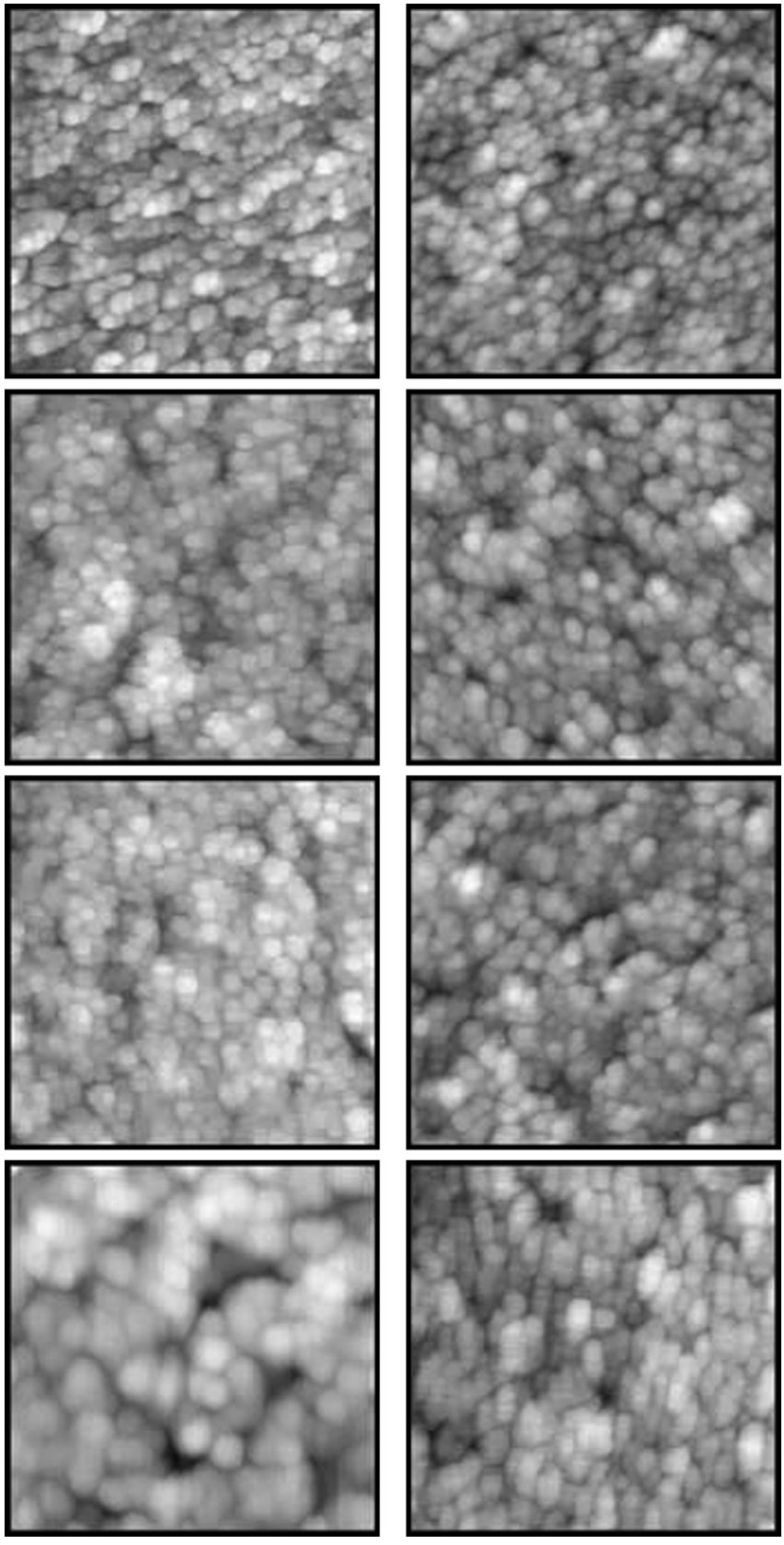

Fig. 5. 1 μm × 1 μm AFM micrographs. Left side: samples deposited at normal incidence. Right side: samples deposited at oblique angle. Power increases from top to bottom.

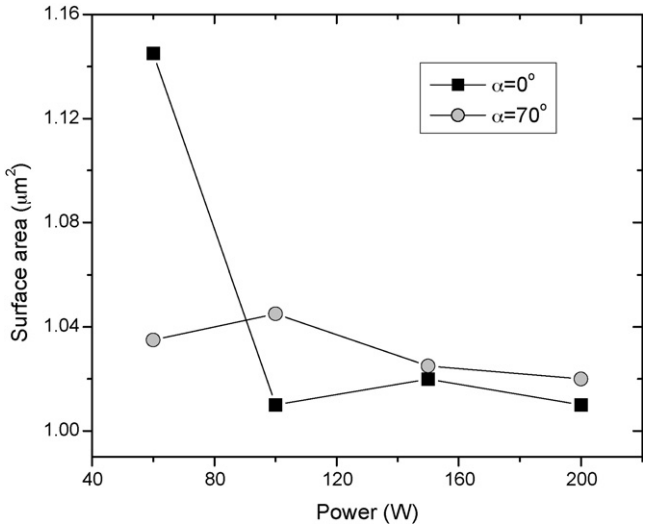

Fig. 6. Surface area as a function of power.

the X-ray diffraction experiments did not show any diffraction peaks, indicating the absence of long-range order. Fig. 5 presents the AFM micrographs. The mean grain size, calculated using the software Image Pro Plus, increases from ∼30 to ∼70 nm with the increase of power, for the samples deposited at normal incidence. For samples deposited at oblique angle, the mean grain size is nearly constant (∼50 nm). From the AFM measurements, the surface area, which is an important parameter to calculate the effective volumetric charge capacity in an electrochemical process, was calculated (Fig. 6). For samples deposited at normal incidence the surface area decrease by 16% with the increase of power. The samples deposited at oblique angle did not show a significant change on this parameter.

Figs. 7 and 8 presents the cross-section micrographs for samples deposited at normal incidence or at 70°, respectively. The samples deposited at normal incidence presents a columnar structure, the top of the columns being larger than the base (funneled form). With the increase of power, the top of the columns increase, causing the increase of the mean grain size observed by AFM. For samples deposited at 70°, the columns are inclined,

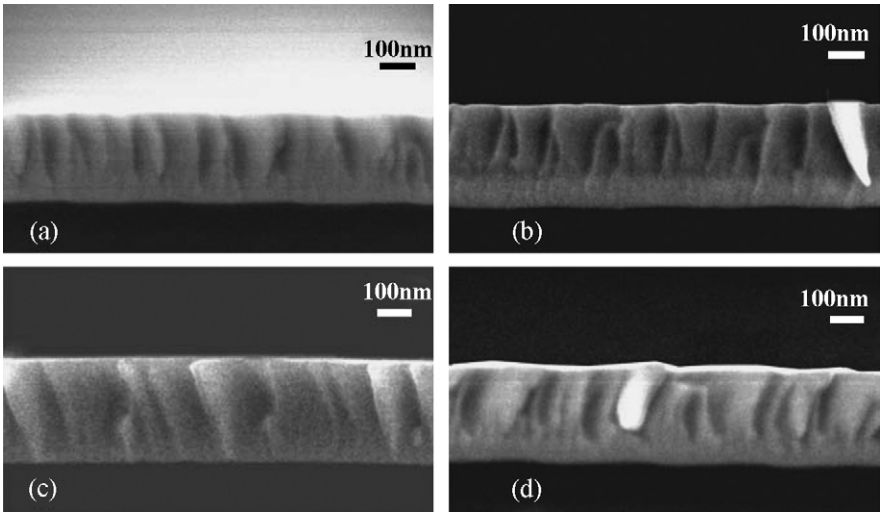

Fig. 7. Cross-section micrographs for samples deposited at normal incidence.

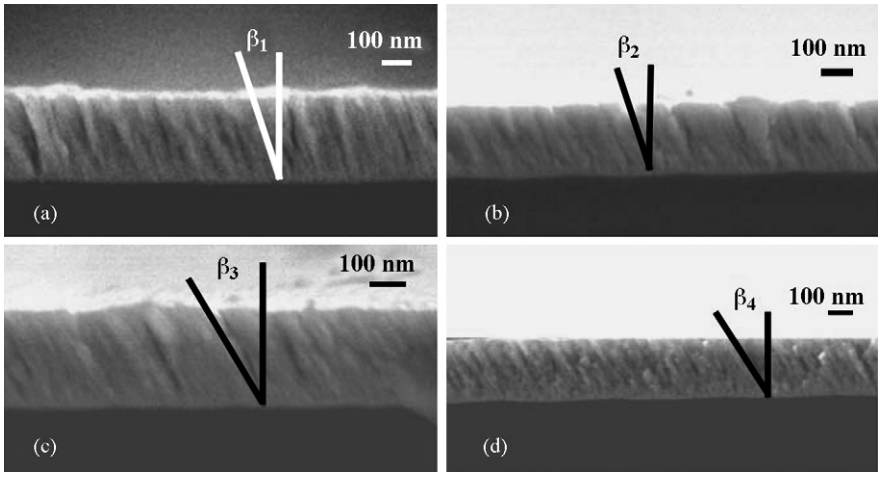

Fig. 8. Cross-section micrographs for samples deposited at oblique incidence.

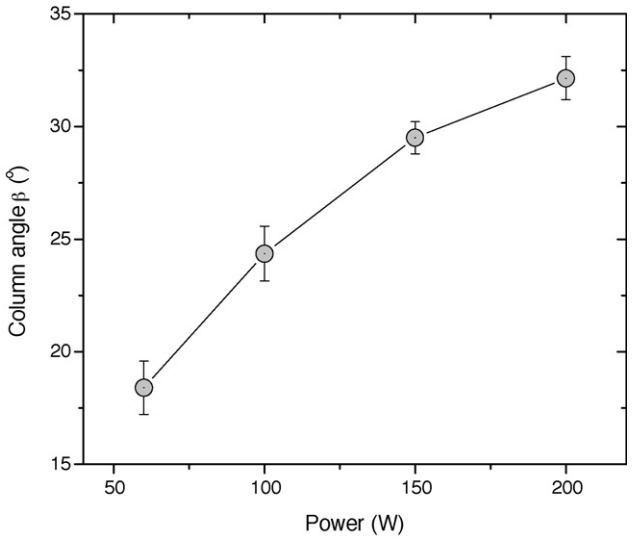

Fig. 9. Columnar angle of inclination with respect to the normal to the substrate vs. power, for samples deposited at oblique incidence.

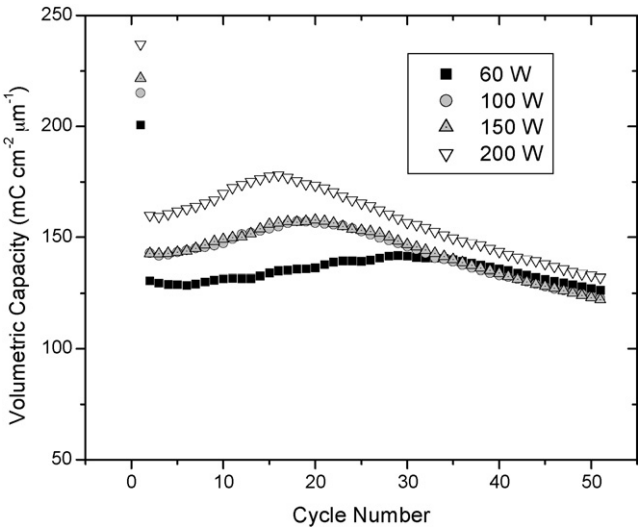

Fig. 11. Charge capacity as a function of the cycle number for the samples deposited at normal incidence.

the angle of inclination with respect to the normal to the substrate (β) increasing from $\beta = 18^\circ$ (60 W) to $\beta = 32^\circ$ (200 W) (Fig. 9). The increase in column angle causes an increase in the porosity of the samples [13,15].

The results concerning the electrochemical behavior of the samples are presented in the following. Fig. 10 presents the behavior of the potential as a function of time, for the first cycle. These chronopotentiometric curves are monotonic, and the characteristics plateaus related to phase transitions are absent, which is typical of amorphous materials. Fig. 11 presents the charge capacity as a function of the cycle number for the samples deposited at 0°. These data are the ratio of the charge inserted during the cathodic process, for each cycle, and the product of the thickness and the geometric area. The charge capacity for the sample deposited at the low power (60 W) presents the lowest values, for all cycles, in spite of the fact that the surface area is 16% greater for this sample, in comparison with other samples of this series. Clearly this is not an effect of surface area. On the other hand, the sample deposited at low power presents the lowest mean grain size (~30 nm); samples deposited at intermediate power present similar grain sizes (~45 nm) and similar charge capacity levels (Fig. 11). The sizes of the microstructure observed by MEV are also similar for these samples (Fig. 7). The samples deposited at the highest power presents the greatest grain and the highest charge capacity values. These data indicates a correlation between grain size and charge capacity. Even if lithium insertion in tungsten oxide films is a well studied intercalation process [6], at the best of our knowledge there are not published works on the correlations of microstructure and the intercalation process. The different grain sizes also implies a different grain boundary distribution, which can affect the intercalation process. Interestingly, the charge capacity first increases with cycling, and then decreases. For the sample deposited at low power, the capacity increase till the 30est cycle; for samples deposited at high power this increase ends at the 15est cycle. The data seems to indicate that the diffusion coefficient is different for the different samples, being higher for the samples deposited at high power. The increase of charge capacity can then be associated with a progressive movement of the lithium diffusion plane [16], (diffusion "front"), that attains deeper regions of the active material at each subsequent cycle, and is slower for samples that present a larger number of grain boundaries. The subsequent decrease of charge capacity is commonly observed in intercalation materials, and is generally associated to a global change of the film structure due to ion trapping [17,18].

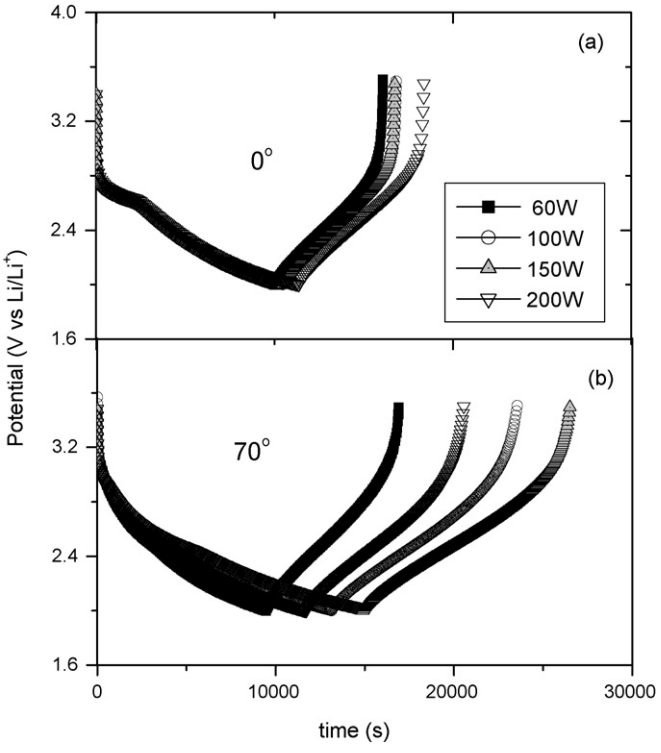

Fig. 10. Potential as a function of time, for the first cycle.

Fig. 12 presents the charge capacity behavior for the samples deposited at oblique angle. The capacity is larger for the samples

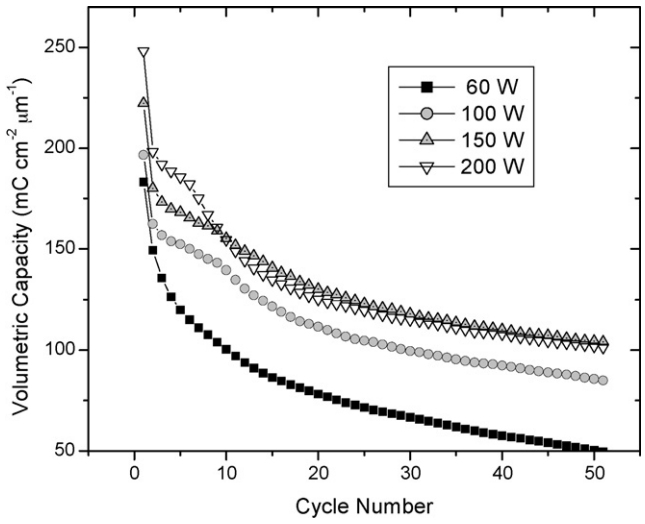

Fig. 12. Charge capacity as a function of the cycle number for the samples deposited at oblique incidence.

deposited at high power, which presents a more porous structure due to the highest inclination of the columns. The porosity facilitates mass exchange, and the capacity decreases continuously with cycling. In this case, a diffusion "front" is not expected.

4. Conclusion

In this work, the deposition conditions of tungsten oxide films have been controlled in order to attain different microstructures. Both the power during deposition, and the inclination of the substrate were varied. The increase of power is beneficial to the charge capacity values. In the normal deposition series, the different grain sizes and, consequently, the different number of grain boundaries, seems to be determinant in the insertion/extraction process. For oblique incidence the inclination of the columns causes porosity, witch facilitates the electrochemical process. In both cases, the charge capacity values can be varied, indicating that an alternative way of optimizing cathode properties for thin film batteries.

Acknowledgements

One author (R.F.) thanks CNPq (Brazil) for financial support. Dr. Airton Lourenço is acknowledged for his help in the experiments. Drs. L.P. Cardoso and M.H. Tabacniks are acknowledged for the XRD and RBS experiments. The FEG-SEM experiments were performed at the Laboratório Nacional de Luz Síncrotron (LNLS, Campinas, Brazil).

References

[1] S. Passerini, B.B. Owens, J. Power Sources 97/98 (2001) 750–754.
[2] C. Julien, G.A. Nazri, Solid-State Batteries, Kluwer Academic Publishers, MA, USA, 1994.
[3] M. Balkanski, Sol. Energy Mater. Sol. Cells 62 (2000) 21–35.
[4] P. Birke, W. Weppner, Electrochim. Acta 42 (1997) 3375–3384.
[5] J.L. Souquet, M. Duclot, Solid State Ionics 148 (2002) 375–379.
[6] C.G. Granqvist, Handbook of Inorganic Electrochromic Materials, Elsevier Science, Amsterdam, 1995.
[7] C.G. Granqvist, A. Azens, A. Hjelm, L. Kullman, G.A. Niklasson, D. Rönnow, M.S. Mattsson, M. Veszelei, G. Vaivars, Sol. Energy 63 (1998) 199–216.
[8] M.K. Aydinol, A.F. Kohan, G. Ceder, K. Cho, J. Joannopoulos, Phys. Rev. B 56 (1997) 1354–1365.
[9] B.B. Owens, W.H. Smyrl, J.J. Xu, J. Power Sources 81/82 (1999) 150–155.
[10] K. Brandt, Solid State Ionics 69 (1994) 173–183.
[11] F. García-Alvarado, M.E. Arroyo y de Dompablo, E. Morán, M.T. Gutiérrez, A. Kuhn, A. Várez, J. Power Sources 81/82 (1999) 85–89.
[12] B. Scrosati, S. Panero, P. Reale, D. Satolli, Y. Aihara, J. Power Sources 105 (2002) 161–168.
[13] K. Robbie, J.C. Sit, M.J. Brett, J. Vac. Sci. Technol. B 16 (1998) 1115–1122.
[14] RUMP/GENPLOT. Computer Graphics Service, 2002.
[15] L. Dong, R.W. Smith, D.J. Srolovitz, J. Appl. Phys. 80 (1996) 5682–5690.
[16] P.J. Bouwman, B.A. Boukamp, H.J.M. Bouwmeester, P.H.L. Notten, Solid State Ionics 152/153 (2002) 181–188.
[17] Y. Sakurai, S. Okada, J. Yamaki, T. Okada, J. Power Sources 20 (1987) 173–177.
[18] J.-G. Zhang, M. McGraw, J. Turner, D. Ginley, J. Electrochem. Soc. 144 (1997) 1630–1634.